HHS Public Access

Author manuscript

Cardiovasc Innov Appl. Author manuscript; available in PMC 2021 September 21.

Published in final edited form as:

Cardiovasc Innov Appl. 2019 April ; 4(1): 13–24. doi:10.15212/cvia.2019.0004.

Emerging Techniques for Cardiovascular PET

Austin A. Robinson, MD[1], **Jamieson M. Bourque, MD,MHS**[1,2]

[1]Cardiovascular Division and the Cardiovascular Imaging Center, Department of Medicine, University of Virginia Health System, Charlottesville, VA

[2]Department of Radiology, University of Virginia Health System, Charlottesville, VA

Abstract

The application of positron emission tomography (PET) to cardiac disease has yielded tremendous developments in the evaluation of coronary artery, myocardial, and valvular heart disease over the past several decades. These advances have included development of new radiotracers, incremental technological improvements, and coupling of PET with other non-invasive cardiac imaging modalities. The current era has seen rapid, successive and wide-ranging advances in PET myocardial perfusion and metabolic imaging. This review will address emerging techniques in cardiovascular PET imaging, including the measurement of absolute myocardial blood flow (MBF), use of novel tracers, and other advances in heart failure, infection imaging, and valvular disease.

CAD Evaluation: Absolute Flow Quantification

A chief contribution of PET to cardiovascular medicine is in the area of myocardial perfusion imaging (MPI). The favorable kinetics of the primary PET perfusion radiotracers, ^{82}Rb and $^{13}NH_3$, and high temporal resolution have enabled the quantification of regional and global MBF (1). The incorporation of MBF into clinical decision-making has yielded substantive improvements in the clinical management of chest pain and coronary artery disease (CAD) and has yielded new data on coronary physiology with far-reaching clinical significance.

Epicardial CAD

Quantification of MBF by PET addresses a shortcoming of single photon-emission computed tomography (SPECT) MPI; in SPECT, the images must be normalized to the region with the highest uptake of radiotracer. This reliance on relative perfusion differences renders SPECT MPI poorly sensitive to global reductions in perfusion in the setting of high-risk multivessel obstructive CAD-- termed “balanced” ischemia because abnormal areas are inappropriately scaled to the normal range (2). Global reductions in absolute flow provide a straightforward means to identify balanced ischemia. Moreover, measurement of MBF, coupled with the higher spatial resolution of PET, also facilitates evaluation of

Address for Correspondence: Jamieson M. Bourque, M.D., M.H.S., Associate Professor of Medicine and Radiology, Cardiovascular Division, Department of Medicine, University of Virginia Health System, Box 800158 ,1215 Lee Street, Charlottesville, VA 22908, Office: (434) 243-9337, Fax: (434) 982-1998, jbourque@virginia.edu.

complex epicardial CAD by allowing for accurate simultaneous assessment of the functional significance of multiple coronary lesions (3). MBF can be compared against visual perfusion defects to more reliably distinguish artifacts from true perfusion defects. In addition to its advantages in diagnosis, measurement of MBF has prognostic importance as well. In patients with abnormal perfusion, an abnormal MPR portends a higher risk of death and major adverse cardiovascular events (4).

Coronary Microvascular Dysfunction

Beyond improving the diagnosis of epicardial obstructive CAD, quantitative MBF during PET MPI has opened new possibilities in the diagnosis, evaluation, and management of coronary microvascular dysfunction (CMD). Myocardial perfusion reserve (MPR), calculated as the ratio of hyperemic MBF to resting MBF has been used as a surrogate for coronary flow reserve (5). An abnormally-low MPR in the absence of obstructive epicardial CAD provides evidence of CMD, giving PET MPI a key role in the diagnosis and monitoring of this disease (6). PET MPR evaluation has application in obese and diabetic patients and has an emerging role in monitoring for chemotherapy-related cardiotoxicity (7, 8). Furthermore, PET MPR analysis can be used over time to non-invasively monitor efficacy of therapies suggested for the treatment of CMD, a critical step for ongoing research and maturation of the field (9).

Coronary Allograft Vasculopathy

Evaluation of coronary allograft vasculopathy (CAV) has historically relied on invasive angiography and intravascular ultrasound. Traditional noninvasive testing options such as dobutamine stress echocardiography and SPECT MPI have demonstrated inadequate specificity for CAV, only moderate sensitivity for obstructive CAV, and inadequate sensitivity for early or non-obstructive CAV (10). Emerging data suggest that PET MPI with quantitative MBF may be able to effectively assess this disease process noninvasively. In 40 post-transplant patients in whom invasive evaluation was used as a gold-standard, ^{82}Rb PET-derived stress MBF, MPR (adjusted for the rate-pressure product) and increased coronary vascular resistance (CVR, calculated as the stress systolic blood pressure divided by stress MBF) all improved the detection of CAV. Using diagnostic cutoffs of MPR <2.9, stress MBF <2.3, and CVR >55, the presence of any 2 parameters demonstrated a diagnostic specificity of 97% and sensitivity of 56 – 68%, depending on the set of parameters (11). While these findings await necessary validation in larger studies, they certainly give reason for optimism regarding the ability of PET to aid in monitoring for CAV in heart transplant recipients.

Obesity with High Resting Flows

Due to the increased count sensitivity, robust attenuation correction, and MBF analysis, PET MPI has decreased susceptibility to soft-tissue-related attenuation artifacts and has become the MPI modality of choice for patients with elevated body mass index (BMI) > 40 (12). This referral pattern has encouraged careful evaluation of the relationship of MBF with elevated BMI. A study of 827 patients without obstructive epicardial CAD who underwent PET MPI found that MPR is inversely correlated with BMI above a BMI cutoff of 30, suggesting that CMD worsens with increasingly-severe obesity (8). Importantly, MPR in this

population was an independent predictor of adverse cardiovascular events, discriminating risk better than BMI and traditional cardiovascular risk factors. Further studies into obesity-specific idiosyncracies of myocardial perfusion, such as the subset of obese patients with high resting MBF, may lead to better risk classification, improved monitoring and potentially allow for improved therapy development in a heretofore understudied patient population.

Diabetes Mellitus

PET MPI is also of value in evaluating another high-risk patient subset: those with diabetes mellitus. This is of particular interest, due to the higher risk of epicardial CAD as well as coronary endothelial dysfunction (13, 14). In a large retrospective cohort of patients undergoing PET MPI, an impairment in MPR (below the median) in diabetes patients was associated with an increased risk of cardiac death, similar in magnitude to the presence of CAD in non-diabetic patients (15). Given the prognostic information added by MBF quantification and added diagnostic accuracy for balanced ischemia, PET MPI may provide added benefit over techniques for first-line ischemic testing in patients with diabetes mellitus. Consequently, a trial evaluation comparing initial ischemic testing strategies for diabetic patients should be contemplated.

CAD Evaluation: Other Advances

New tracers: Flurpiridaz

Although they are significantly improved over existing SPECT tracers, ^{82}Rb and $^{13}NH_3$ have limitations. Both ^{82}Rb and $^{13}NH_3$ have suboptimal myocardial extraction at higher flow rates, leading to a misestimation of MBF (Figure 1). Moreover, their short half-lives create a need for specialized production procedures. $^{13}NH_3$ is created in a cyclotron that must be locally situated due to the 10-minute half-life of this tracer. Likewise,^{82}Rb has a half-life of 82 seconds and must be eluted from a ^{82}Sr generator while the patient is in the PET scanner (16). These limitations have spurred development of ^{18}F -BMS-747158–02 (^{18}F -Flurpiridaz), a radiotracer with high mitochondrial binding that can be used for PET MPI (17). Importantly, the longer half-life of the ^{18}F moiety eliminates the requirement for an on-site cyclotron, allowing a marked expansion of the stress labs capable of using this tracer. Moreover, the longer half-life permits delayed imaging post-injection, a prerequisite for combination with exercise stress. In addition to these benefits, ^{18}F-Flurpiridaz maintains myocardial uptake at high coronary flow rates with less roll-off compared with both ^{82}Rb and $^{13}NH_3$ tracers. ^{18}F -Flurpiridaz is under evaluation in the ongoing AURORA study (NCT03354273), a phase 3 trial evaluating the diagnostic performance of ^{18}F -Flurpiridaz compared with SPECT and invasive coronary angiography. If results are consistent with prior data with the tracer, ^{18}F -Flurpiridaz may well be positioned to address the three most significant limitations of current PET myocardial perfusion tracers: tracer availability, uptake fidelity at high flow rates, and compatibility with exercise stress testing.

An interesting conundrum arising from the use of ^{18}F -Flurpiridaz is its compatibility with exercise stress and ability to provide absolute flow quantification—but not both simultaneously. The time gap between the end of exercise and the start of scanning prevents reliable measurement of absolute MBF. The inability to perform both exercise

stress and absolute flow assessment forces a choice between two important diagnostic and prognostic parameters. Exercise stress provides exercise capacity (the most powerful stress prognostic marker), hemodynamic response and potential for symptom reproduction while increasing the diagnostic accuracy of the ST-analysis. Absolute flow measurement provides rich data from resting MBF, hyperemic MBF and MPR. Rather than omitting one or another important dataset, we propose a hybrid protocol in which exercise stress is performed to gather stress ECG, hemodynamic, and symptom data followed by on-table vasodilator stress to allow for absolute blood flow quantification (Figure 2)

Plaque Characterization

The utility of cardiac PET in CAD extends beyond the evaluation of myocardial ischemia. Cardiac PET with molecular imaging tracers allows for functional interrogation of vascular biology and characterization of atherosclerotic plaques.

^{18}F-Fluorodeoxyglucose—^{18}F-fluorodeoxyglucose (^{18}F-FDG) activity correlates with arterial inflammation due to uptake by metabolically-active macrophages (18). However, examination of the coronary arteries for inflammation with ^{18}F-FDG is hampered by the proximity of coronary arteries to the myocardium, which may have concurrent ^{18}F-FDG uptake. While introducing a low-carbohydrate, high-fat diet may be helpful in suppressing myocardial ^{18}F-FDG uptake (19), distinguishing coronary from patchy myocardial uptake remains difficult, even with effective myocardial suppression (20). Underscoring these technical concerns, ^{18}F-FDG has demonstrated a low diagnostic performance, with an inability to identify culprit coronary lesions in nearly half of a group of patients presenting with an acute coronary syndrome (21).

^{18}F-Sodium Fluoride—The difficulties with using ^{18}F-FDG for non-invasive plaque characterization have led to the pursuit of alternative tracers. ^{18}F-Sodium fluoride (^{18}F-NaF) has been identified as a marker of valvular and vascular calcification, including the microcalcifications present in the necrotic core of vulnerable, thin-cap fibroatheromas (Figure 3) (22). In an early clinical study, ^{18}F-NaF outperformed ^{18}F-FDG in localizing coronary signal and in distinguishing culprit from non-culprit coronary plaques (20). ^{18}F-NaF is the subject of an ongoing, prospective outcomes study to validate its utility in predicting high risk plaques (NCT02278211). However, the question of ideal PET radiotracer to characterize vascular plaques is not yet settled.

^{68}Ga-DOTATATE—Another promising radiotracer for the evaluation of plaque inflammation has emerged in ^{68}Ga- [1,4,7,10-tetraazacyclododecane-N,N’,N“,N”’-tetraacetic acid]-D-Phe^{1}, Tyr^{3}-octreotate (^{68}Ga-DOTATATE). ^{68}Ga-DOTATATE binds with high affinity to type 2 somatostatin receptors, whose expression is upregulated on the surface of activated tissue macrophages (23). In an early clinical study, ^{68}Ga-DOTATATE demonstrated fairly good performance in the identification of culprit plaques after acute coronary syndrome, with a sensitivity of 87.5%, specificity of 78.4%, and receiver operator characteristic (ROC) area under of the curve (AUC) for diagnostic accuracy of 0.86 (24). Furthermore, ^{68}Ga-DOTATATE signal was higher in non-culprit plaques with high risk morphologic features (spotty calcification, low attenuation, or positive remodeling). In

addition to clinical trials, an important next step for plaque-focused radiotracers would include prospective cohort studies, with comparison against other risk stratifiers such as coronary calcium scoring to evaluate reclassification potential.

Heart Failure

Risk Stratification by Viability Assessment

Cardiac PET plays a major role in the evaluation and management of heart failure. Both SPECT and PET MPI are well-established methods of detecting ischemia as a cause of heart failure (25). However, PET can provide additional risk stratification for patients with heart failure through absolute flow quantification and metabolic imaging. Ghannam et al. examined a cohort of 159 patients with implantable cardioverter defibrillators (ICDs) who underwent ^{82}Rb PET MPI. They found that PET stress MBF, but not summed rest or stress scores, predicted the risk of ventricular tachycardia or ventricular fibrillation (26). However, it is the combination of perfusion information with metabolic imaging that brings cardiac PET to the forefront of heart failure evaluation. Metabolic assessment by ^{18}F FDG PET is widely regarded as a gold standard for viability over other modalities that draw conclusions based on resting perfusion uptake (25). The presence of viable myocardium by PET predicts functional improvement after revascularization (27). Additionally, there is evidence that PET-guided care may improve outcomes. In the PARR-2 randomized trial of PET viability-guided vs standard care for evaluation of severely reduced LVEF, the subgroup of patients from the PET arm whose care adhered to the PET-guided revascularization recommendations experienced a lower rate of composite adverse events (28).

Risk Stratification by Sympathetic Denervation: ^{11}C-HED

Risk stratification is increasingly important for non-ischemic heart failure in addition to patients with CAD. Recent trial data indicate that a left ventricular ejection fraction (LVEF) ≤ 35% is an insufficient marker for predicting the risk of sudden cardiac death in patients with non-ischemic cardiomyopathy, underscoring the need for additional prognostic markers in this large patient population (29). While there is likely a role for late gadolinium enhancement by cardiac magnetic resonance (CMR), accumulating data suggest that PET has predictive power regarding sudden cardiac death (30). The use of ^{11}C-hydroxyephedrine (C-HED), an analog of norepinephrine, has allowed non-invasive evaluation of cardiac sympathetic innervation. C-HED binds selectively in the heart to pre-synaptic sympathetic nerve terminals (31). Regions of cardiac denervation and dysautonomia demonstrate reliably-reduced C-HED uptake compared to controls (32). In a prospective trial of patients with ischemic HFrEF, sudden cardiac arrest was predicted by the amount of sympathetically denervated myocardium but not LVEF or infarct size (33).

Delineation of inflammatory/infiltrative cardiomyopathies

Cardiac Amyloid:^{11}C-PIB , florbetapir, florbetaben—Cardiac PET has shown promise in the delineation of non-ischemic cardiomyopathy type as well. Among non-ischemic cardiomyopathies, the identification of cardiac amyloidosis is particularly important due to the aggressive course of disease, difficulties in non-invasive evaluation, and new effective treatments (34–36). Moreover, traditional diagnostic methods, such as

electrocardiography and 2-dimensional echocardiography, are inadequately sensitive (37, 38). By contrast, cardiac PET, like ^{99m}Tc SPECT, offers the ability to directly diagnose amyloid deposits. There is early evidence that hybrid PET with cardiac magnetic resonance (MR) allows for the distinction between transthyretin and light-chain amyloid variants (see section on hybrid imaging).

Modifications of the amyloid-binding dye Thioflavin T led to the identification of ^{11}C-Pittsburgh Compound B (^{11}C-PIB), structurally N-methyl-[^{11}C]2-(4′-methylaminophenyl)-6-hydroxybenzothiazole. Originally developed for detection of brain amyloid deposition in patients with Alzheimer's disease, it became apparent that ^{11}C-PIB lent itself to the identification of cardiac amyloid involvement as well

(39). ^{11}C-PIB myocardial PET appears to identify myocardium infiltrated by both light chain (AL) and transthyretin (TTR) amyloid with great specificity (40). Other radiotracer have also been shown promise in identifying cardiac amyloid fibrils: ^{18}F-florbetapir and ^{18}F-florbetaben (41, 42). Like ^{11}C-PIB , ^{18}F-florbetapir and ^{18}F-florbetaben were also originally developed to bind brain amyloid.

In the aggregate, cardiac PET for cardiac amyloid appears to have a remarkably robust diagnostic performance. A recent meta-analysis of cardiac PET for the diagnosis of amyloid, aggregating data on 98 subjects across 6 studies (4 of ^{11}C-PIB and 1 each of ^{18}F-florbetapir and ^{18}F-florbetaben), estimated a pooled sensitivity of 0.95 and specificity of 0.98 (43). While promising, much work needs to be done, including analysis in larger groups with broader cardiac disease profiles and development of standardized semi-quantitative parameters and reference ranges before PET can be adopted into clinical practice for patients with suspected cardiac amyloidosis. Additionally, the integration of molecular imaging with new amyloid-targeted therapeutics remains a largely unanswered question. For example, in the pivotal clinical trial of tafamidis for patients with transthyretin amyloid cardiomyopathy, much of the benefit seemed clustered in the subgroup of patients with less severe heart failure, according to symptomatic classification (35). These results suggest there may be different disease stages with varying degrees of treatment susceptibility. In such a situation, it would be reasonable to expect targeted molecular imaging with PET to provide finer stratification of disease profiles to guide treatment selection.

Cardiac Sarcoid: ^{18}F-FDG—Its central role in cardiac sarcoidosis is a chief example of how cardiac PET can be used to diagnose and monitor non-ischemic cardiomyopathies (44). Performed in the setting of a low-carbohydrate, high-fat diet to suppress physiologic myocardial uptake, ^{18}F-FDG PET can identify abnormal glucose uptake indicative of inflammation within the myocardium; in the appropriate clinical scenario, this is consistent with active cardiac sarcoidosis (45). When paired with MPI using a conventional perfusion tracer such as ^{13}N-ammonia or ^{82}Rb to assess myocardial scar from ongoing severe active inflammation or prior disease, cardiac PET offers the ability to provide a comprehensive assessment of the extent of cardiac sarcoid involvement.

Already a cornerstone of sarcoid diagnosis, ^{18}F-FDG PET continues to have technical improvements to improve diagnostic accuracy. One ongoing development is the addition

of ^{18}F-FDG activity quantification to visual assessment. A common semi-quantitative technique employed in PET uses standardized uptake values (SUVs), which are calculated by dividing the tracer uptake (corrected for decay) by the weight-based dose of the tracer (46). Common research approaches have involved measuring the maximum SUV and mean SUV throughout the myocardium (47, 48). Another quantitative approach has been developed based on oncologic PET imaging, wherein the aggregate volume of ^{18}F-FDG-positive myocardium is quantified (49). This volume, called cardiac metabolic volume (CMV), is analogous to metabolic tumor volume in oncology. Calculating CMV allows for determination of the volume-intensity product, dubbed cardiac metabolic activity (CMA), which is analogous to total lesion glycolysis in oncology. In a small study comparing CMA with CMV and maximum SUV, CMA had the best diagnostic performance for ^{18}F-FDG and showed the potential for reclassification (49). As with all new quantitative measures, thresholds, methods of automation, and processing techniques need to be optimized and standardized.

Infection

The ability of ^{18}F-FDG PET to visualize inflammatory metabolic signal has been utilized in the past to identify infections involving vascular prostheses (50). More recently, this technique has been applied in infection imaging related to the heart as well.

Pacemakers and ICDs

It appears that there is increased ^{18}F-FDG uptake in the region of infected ICD and permanent transvenous pacemaker cans and leads (51). A small, prospective study suggests favorable test characteristics for pocket infections, with a sensitivity of 86.7% and specificity of 100% (52). The performance of cardiac PET for device-related endocarditis was much less robust, with a sensitivity of 30.8% and specificity of 62.5%; there were a large number of false negatives (9 of 13 subjects). Previous antimicrobial treatment was the presumed explanation for 8 of the 9 false negatives. The ideal role for ^{18}F-FDG in diagnosing pocket infections has yet to be fully determined. Accordingly, current recommendations by the Heart Rhythm Society provide a class IIb indication for ^{18}F-FDG PET to facilitate the diagnosis of device infection when it cannot be confirmed by other methods (53). Future studies should provide comparisons between relevant patient groups (e.g. antibiotic naïve) and address cost effectiveness.

LVADs

Similar to the uptake seen with pacemakers and ICDs, other intra-cardiac and device-related infections appear to show increased ^{18}F-FDG signal on PET. For instance, the identification of prosthesis infection can be critical in the case of LV assist devices (LVADs), where the patient is fully-dependent on the device for survival and extraction is risky and fraught with complications. Given this importance, it is promising that a study of 35 LVAD patients with suspected device infection (a reasonable population size given the rate nature of this condition) showed that ^{18}F-FDG PET added substantially to the diagnostic work-up. Of 35 individuals, ^{18}F-FDG identified potential infection in 28 patients, compared to only 4 based on CT results alone (54). Additionally, PET was able to establish whether the pattern of

infection was limited to peripheral components or involved the central apparatus. Cardiac PET in LVADs was found to be prognostically important. None of the patients with no evidence of infection on PET imaging died over a mean 23 months of follow-up compared with 50% of patients with evidence of infection (p=0.03).

Infective Endocarditis

Application of infection imaging in infective endocarditis (IE) is challenging due to the intricate nature of the criterion-based diagnosis. One creative approach has been to include ^{18}F-FDG uptake at the site of a prosthetic valve as a major criterion in the Duke IE classification scheme. In a prospective study, including ^{18}F-FDG PET in the updated scoring system increased the sensitivity to 97% from 73% without PET in the classification scheme (55). In a meta-analysis of 13 studies that included prosthetic and native-valve IE, the pooled sensitivity and specificity of hybrid PET/computerized tomography (CT) for IE was 76.8% and 77.9% respectively (56). Concerns persist about limitations in the specificity of this technique, however, as increased ^{18}F-FDG signal can result from post-operative inflammatory changes after recent surgery, vasculitis, active thrombi, cardiac tumors/metastasis and foreign body reactions (57). A reasonable next step is a larger scale trial of patients without post-operative confounders and cost effectiveness analysis.

Valvular Disease

In the realm of valvular heart disease, cardiac PET has been applied beyond the assessment of IE. The properties that have allowed use of ^{18}F-NaF as a marker of calcification within atherosclerotic vascular plaques has also led to its use in the evaluation of calcific heart disease. In a prospective study of 81 subjects with echocardiographically-diagnosed aortic stenosis (AS), 91% demonstrated increased ^{18}F-NaF uptake. Tracer uptake correlated with severity of AS (46). In a 1-year follow-up study with hybrid CT imaging, isolated ^{18}F-NaF uptake in a segment predicted the subsequent development of calcification (58). This development suggests that ^{18}F-NaF can track the development of valvular processes before development of irretrievable damage, which has implications for disease monitoring and evaluation of preventive therapies. Accordingly, ^{18}F-NaF uptake by PET is being used to track progression of AS in an ongoing clinical trial of bisphosphonates and RANK-ligand inhibitors (NCT02132026). It follows from these data that ^{18}F-NaF could also potentially be applied in the evaluation of mitral annular calcification, an under-studied and increasingly frequent cause of mitral valve disease (59).

Technical Advances

Hybrid Imaging

A complete discussion of the uses of hybrid PET/anatomic imaging is beyond the scope of this work, but hybrid imaging has become a critical component of many of the techniques discussed, including MPI, plaque characterization and infection imaging. Combination non-contrast CT with PET MPI allows for attenuation correction and enhanced risk stratification with coronary artery calcium scoring (60). The addition of PET MPI to coronary CT angiography markedly increases diagnostic specificity for obstructive CAD (from 66% to

93%, according to a recent meta-analysis) (61). Likewise, cardiac MR and PET provide synergistic information. By co-localizing areas of FDG uptake by PET with subepicardial late gadolinium enhancement and T2 mapping by CMR, hybrid PET/MR can provide refinements in the evaluation of myocarditis (62). Whether this approach can improve on the performance of establish diagnostic criteria for myocarditis remains to be seen (63). The addition of MR to PET perfusion and metabolic imaging can provide more refined cardiac sarcoid staging than with either modality alone, but the relevance of this for functional outcomes needs to be further defined (64). Finally, a recent study has suggested that hybrid PET/MR may allow distinction of cardiac amyloid subtypes. The findings suggest that co-localized ^{18}F-NaF and late gadolinium enhancement is observed in myocardial regions infiltrated by transthyretin—but not light-chain—amyloid (65).

Machine Learning

Hybrid imaging, with its roots in combining and integrating different data sets, is an area ripe for benefit from machine learning. Typically applied to numerical data sets, machine learning is positioned to aid in processing the inherent complexity of hybrid imaging techniques, as well as demographic and clinical information within electronic health records (66). Further, machine and deep learning are expected by some investigators to allow for fully-automated quantification and image interpretation (67). This has implication for artifact identification, workflow streamlining and efficiency and minimizing inter-reader variability.

Total Body PET

A pending innovation with far-reaching implications for myocardial PET assessment is the current effort to develop a total body PET scanner. Total body PET, consisting of detector rings that span the length of the body, has the potential to provide dramatic technical improvements by allowing signal detection from regions outside the traditional scanner field of view. Further, it allows collection of substantially more signal from a region of interest (ROI) such as the heart. In current PET scanners, only 3–5% of available signal from the ROI intercepts with the limited detector rings (68). Use of total body PET is expected to yield a roughly 40-fold increase in the sensitivity for whole body imaging, though less for the heart itself. This can enable proportionate reductions in the required radiation doses, which can in turn broaden application of cardiac PET techniques to younger populations and provide greater tolerance for serial scanning when necessary. The pending development of the first total body PET scanner for human use is highly anticipated.

Conclusion

From its origin in diagnosing coronary artery stenoses, cardiovascular PET has grown into a staple of contemporary cardiovascular care with impending advances touching all corners of the field, including new tracers and absolute flow assessment in CAD and CMD and characterization of lesions in vascular plaques, cardiac valves, the myocardium and implanted devices (Figure 4). In addition to its breadth of application, cardiovascular PET offers critical diagnostic information, informs prognosis and has the potential to impact care.

Given these strengths and ongoing advances, the present of cardiovascular PET is bright and its future potential enormous.

References

1. Murthy VL, Bateman TM, Beanlands RS, et al.Clinical quantification of myocardial blood flow using PET: Joint position paper of the SNMMI cardiovascular council and the ASNC. Journal of Nuclear Cardiology. 2018;25:269–97. [PubMed: 29243073]
2. Lima RS, Watson DD, Goode AR, et al.Incremental value of combined perfusion and function over perfusion alone by gated SPECT myocardial perfusion imaging for detection of severe three-vessel coronary artery disease. J Am Coll Cardiol. 2003;42:64–70. [PubMed: 12849661]
3. Ziadi MC, Williams K, Guo A, et al.Does quantification of myocardial flow reserve using rubidium-82 positron emission tomography facilitate detection of multivessel coronary artery disease?Journal of Nuclear Cardiology. 2012;19:670–80. [PubMed: 22415819]
4. Herzog BA, Husmann L, Valenta I, et al.Long-term prognostic value of 13N-ammonia myocardial perfusion positron emission tomography: Added value of coronary flow reserve. J Am Coll Cardiol. 2009;54:150–6. [PubMed: 19573732]
5. Kaufmann PA, Camici PG. Myocardial blood flow measurement by PET: Technical aspects and clinical applications. The Journal of Nuclear Medicine. 2005;46:75. [PubMed: 15632037]
6. Camici PG, Crea F. Coronary microvascular dysfunction. N Engl J Med. 2007;356:830–40. [PubMed: 17314342]
7. Chintalgattu V, Rees ML, Culver JC, et al.Coronary microvascular pericytes are the cellular target of sunitinib malate-induced cardiotoxicity. Sci Transl Med. 2013;5:187ra69.
8. Bajaj NS, Osborne MT, Gupta A, et al.Coronary microvascular dysfunction and cardiovascular risk in obese patients. J Am Coll Cardiol. 2018;72:707–17. [PubMed: 30092946]
9. Löffler AI, Bourque JM. Coronary microvascular dysfunction, microvascular angina, and management. Curr Cardiol Rep. 2016;18:1. [PubMed: 26694723]
10. Pollack A, Nazif T, Mancini D, Weisz G. Detection and imaging of cardiac allograft vasculopathy. JACC: Cardiovascular Imaging. 2013;6:613–23. [PubMed: 23680373]
11. Chih S, Chong AY, Erthal F, et al.PET assessment of epicardial intimal disease and microvascular dysfunction in cardiac allograft vasculopathy. J Am Coll Cardiol. 2018;71:1444–56. [PubMed: 29598865]
12. Harnett DT, Hazra S, Maze R, et al.Clinical performance of rb-82 myocardial perfusion PET and tc-99m-based SPECT in patients with extreme obesity. Journal of Nuclear Cardiology. 2017:1–9.
13. Di Carli MF, Janisse J, Ager J, Grunberger G. Role of chronic hyperglycemia in the pathogenesis of coronary microvascular dysfunction in diabetes. J Am Coll Cardiol. 2003;41:1387–93. [PubMed: 12706936]
14. Sezer M, Kocaaga M, Aslanger E, et al.Bimodal pattern of coronary microvascular involvement in diabetes mellitus. J Am Heart Assoc. 2016;5:10.1161/JAHA.116.003995.
15. Murthy VL, Naya M, Foster CR, et al.Association between coronary vascular dysfunction and cardiac mortality in patients with and without diabetes mellitus. Circulation. 2012;126:1858–68. [PubMed: 22919001]
16. Sogbein OO, Pelletier-Galarneau M, Schindler TH, Wei L, Wells RG, Ruddy TD. New SPECT and PET radiopharmaceuticals for imaging cardiovascular disease. BioMed research international. 2014;2014.
17. Nekolla S, Reder S, Saraste A, et al.Evaluation of the novel myocardial perfusion positron-emission tomography tracer 18F-BMS-747158–02. Circulation. 2009.
18. Rudd JH, Warburton E, Fryer TD, et al.Imaging atherosclerotic plaque inflammation with [18F]-fluorodeoxyglucose positron emission tomography. Circulation. 2002;105:2708–11. [PubMed: 12057982]
19. Wykrzykowska J, Lehman S, Williams G, et al.Imaging of inflamed and vulnerable plaque in coronary arteries with 18F-FDG PET/CT in patients with suppression of myocardial uptake using a low-carbohydrate, high-fat preparation. J Nucl Med. 2009;50:563–8. [PubMed: 19289431]

20. Joshi NV, Vesey AT, Williams MC, et al.18F-fluoride positron emission tomography for identification of ruptured and high-risk coronary atherosclerotic plaques: A prospective clinical trial. The Lancet. 2014;383:705–13.
21. Cheng VY, Slomka PJ, Le Meunier L, et al.Coronary arterial 18F-FDG uptake by fusion of PET and coronary CT angiography at sites of percutaneous stenting for acute myocardial infarction and stable coronary artery disease. Journal of Nuclear Medicine. 2012;53:575. [PubMed: 22419753]
22. Irkle A, Vesey AT, Lewis DY, et al.Identifying active vascular microcalcification by 18 F-sodium fluoride positron emission tomography. Nature communications. 2015;6:7495.
23. Dalm VA, Van Hagen PM, van Koetsveld PM, et al.Expression of somatostatin, cortistatin, and somatostatin receptors in human monocytes, macrophages, and dendritic cells. American Journal of Physiology-Endocrinology and Metabolism. 2003;285:E344–53. [PubMed: 12684217]
24. Tarkin JM, Joshi FR, Evans NR, et al.Detection of atherosclerotic inflammation by 68Ga-DOTATATE PET compared to [18F] FDG PET imaging. J Am Coll Cardiol. 2017;69:1774–91. [PubMed: 28385306]
25. Garbi M, McDonagh T, Cosyns B, et al.Appropriateness criteria for cardiovascular imaging use in heart failure: Report of literature review. European Heart Journal-Cardiovascular Imaging. 2014;16:147–53. [PubMed: 25550363]
26. Ghannam M, Mikhova K, Yun HJ, et al.Relationship of non-invasive quantification of myocardial blood flow to arrhythmic events in patients with implantable cardiac defibrillators. Journal of Nuclear Cardiology. 2017:1–11.
27. Di Carli MF, Asgarzadie F, Schelbert HR, et al.Quantitative relation between myocardial viability and improvement in heart failure symptoms after revascularization in patients with ischemic cardiomyopathy. Circulation. 1995;92:3436–44. [PubMed: 8521565]
28. Beanlands RS, Nichol G, Huszti E, et al.F-18-fluorodeoxyglucose positron emission tomography imaging-assisted management of patients with severe left ventricular dysfunction and suspected coronary disease: A randomized, controlled trial (PARR-2). J Am Coll Cardiol. 2007;50:2002–12. [PubMed: 17996568]
29. Køber L, Thune JJ, Nielsen JC, et al.Defibrillator implantation in patients with nonischemic systolic heart failure. N Engl J Med. 2016;375:1221–30. [PubMed: 27571011]
30. Salerno M, Robinson AA. Risk stratification in nonischemic dilated cardiomyopathy in the era of personalized medicine: Can cardiac magnetic resonance with late gadolinium imaging “enhance” our strategy?JACC Cardiovasc Imaging. 2018;11:1285–7. [PubMed: 30190029]
31. Schwaiger M, Kalff V, Rosenspire K, et al.Noninvasive evaluation of sympathetic nervous system in human heart by positron emission tomography. Circulation. 1990;82:457–64. [PubMed: 2372893]
32. Luisi AJ Jr, Suzuki G, Haka MS. Regional^ sup 11^ C-hydroxyephedrine retention in hibernating myocardium: Chronic inhomogeneity of sympathetic innervation in the absence of infarction. The Journal of Nuclear Medicine. 2005;46:1368. [PubMed: 16085596]
33. Fallavollita JA, Heavey BM, Luisi AJ, et al.Regional myocardial sympathetic denervation predicts the risk of sudden cardiac arrest in ischemic cardiomyopathy. J Am Coll Cardiol. 2014;63:141–9. [PubMed: 24076296]
34. Falk RH. Diagnosis and management of the cardiac amyloidoses. Circulation. 2005;112:2047–60. [PubMed: 16186440]
35. Maurer MS, Schwartz JH, Gundapaneni B, et al.Tafamidis treatment for patients with transthyretin amyloid cardiomyopathy. N Engl J Med. 2018;379:1007–16. [PubMed: 30145929]
36. Adams D, Gonzalez-Duarte A, O’Riordan WD, et al.Patisiran, an RNAi therapeutic, for hereditary transthyretin amyloidosis. N Engl J Med. 2018;379:11–21. [PubMed: 29972753]
37. Pagourelias ED, Mirea O, Duchenne J, et al.Echo parameters for differential diagnosis in cardiac amyloidosis: A head-to-head comparison of deformation and nondeformation parameters. Circulation: Cardiovascular Imaging. 2017;10:e005588. [PubMed: 28298286]
38. Cheng Z, Zhu K, Tian Z, Zhao D, Cui Q, Fang Q. The findings of electrocardiography in patients with cardiac amyloidosis. Annals of Noninvasive Electrocardiology. 2013;18:157–62. [PubMed: 23530486]

39. Klunk WE, Engler H, Nordberg A, et al.Imaging brain amyloid in alzheimer's disease with pittsburgh Compound-B. Annals of Neurology: Official Journal of the American Neurological Association and the Child Neurology Society. 2004;55:306–19.
40. Antoni G, Lubberink M, Estrada S, et al.In vivo visualization of amyloid deposits in the heart with 11C-PIB and PET. J Nucl Med. 2013;54:213–20. [PubMed: 23238792]
41. Dorbala S, Di Carli MF. In: Cardiac PET perfusion: Prognosis, risk stratification, and clinical management. Seminars in nuclear medicine; Elsevier, 2014. p. 344–57.
42. Law WP, Wang W, Moore PT, Mollee PN, Ng A. Cardiac amyloid imaging with 18F-florbetaben PET: A pilot study. J Nucl Med. 2016;57:1733–9. [PubMed: 27307344]
43. Kim YJ, Ha S, Kim Y. Cardiac amyloidosis imaging with amyloid positron emission tomography: A systematic review and meta-analysis. Journal of Nuclear Cardiology. 2018:1–10. [PubMed: 29043552]
44. Birnie DH, Sauer WH, Bogun F, et al.HRS expert consensus statement on the diagnosis and management of arrhythmias associated with cardiac sarcoidosis. Heart Rhythm. 2014;11:1305–23. [PubMed: 24819193]
45. Soussan M, Brillet P, Nunes H, et al.Clinical value of a high-fat and low-carbohydrate diet before FDG-PET/CT for evaluation of patients with suspected cardiac sarcoidosis. Journal of Nuclear Cardiology. 2013;20:120–7. [PubMed: 23188627]
46. Dweck MR, Jones C, Joshi NV, et al.Assessment of valvular calcification and inflammation by positron emission tomography in patients with aortic stenosis. Circulation. 2012;125:76–86. [PubMed: 22090163]
47. Hulten E, Aslam S, Osborne M, Abbasi S, Bittencourt MS, Blankstein R. Cardiac sarcoidosis-state of the art review. Cardiovasc Diagn Ther. 2016;6:50–63. [PubMed: 26885492]
48. Mc Ardle BA, Birnie DH, Klein R, et al.Is there an association between clinical presentation and the location and extent of myocardial involvement of cardiac sarcoidosis as assessed by 18F-fluorodoexyglucose positron emission tomography?Circulation: Cardiovascular Imaging. 2013;6:617–26. [PubMed: 23884290]
49. Ahmadian A, Brogan A, Berman J, et al.Quantitative interpretation of FDG PET/CT with myocardial perfusion imaging increases diagnostic information in the evaluation of cardiac sarcoidosis. Journal of nuclear cardiology. 2014;21:925–39. [PubMed: 24879453]
50. Keidar Z, Engel A, Hoffman A, Israel O, Nitecki S. 18f-fdg pet/ct. J Nucl Med. 2007;48:1230–6. [PubMed: 17631553]
51. Sarrazin J, Philippon F, Tessier M, et al.Usefulness of fluorine-18 positron emission tomography/computed tomography for identification of cardiovascular implantable electronic device infections. J Am Coll Cardiol. 2012;59:1616–25. [PubMed: 22538331]
52. Cautela J, Alessandrini S, Cammilleri S, et al.Diagnostic yield of FDG positron-emission tomography/computed tomography in patients with CEID infection: A pilot study. Europace. 2012;15:252–7. [PubMed: 23148119]
53. Kusumoto FM, Schoenfeld MH, Wilkoff BL, et al.2017 HRS expert consensus statement on cardiovascular implantable electronic device lead management and extraction. Heart Rhythm. 2017;14:e503–51. [PubMed: 28919379]
54. Kim J, Feller ED, Chen W, Liang Y, Dilsizian V. FDG PET/CT for early detection and localization of left ventricular assist device infection: Impact on patient management and outcome. JACC: Cardiovascular Imaging. 2018.
55. Saby L, Laas O, Habib G, et al.Positron emission tomography/computed tomography for diagnosis of prosthetic valve endocarditis: Increased valvular 18F-fluorodeoxyglucose uptake as a novel major criterion. J Am Coll Cardiol. 2013;61:2374–82. [PubMed: 23583251]
56. Mahmood M, Kendi AT, Ajmal S, et al.Meta-analysis of 18F-FDG PET/CT in the diagnosis of infective endocarditis. Journal of Nuclear Cardiology. 2017:1–14.
57. Habib G, Lancellotti P, Antunes MJ, et al.2015 ESC guidelines for the management of infective endocarditis: The task force for the management of infective endocarditis of the european society of cardiology (ESC) endorsed by: European association for cardio-thoracic surgery (EACTS), the european association of nuclear medicine (EANM). Eur Heart J. 2015;36:3075–128. [PubMed: 26320109]

58. Dweck MR, Jenkins WS, Vesey AT, et al.18F-sodium fluoride uptake is a marker of active calcification and disease progression in patients with aortic stenosis. Circulation: Cardiovascular Imaging. 2014;7:371–8. [PubMed: 24508669]

59. Jenkins WS, Chin C, Rudd JH, Newby DE, Dweck MR. What can we learn about valvular heart disease from PET/CT?Future cardiology. 2013;9:657–67. [PubMed: 24020668]

60. Pan JA, Salerno M. Clinical utility and future applications of PET/CT and PET/CMR in cardiology. Diagnostics. 2016;6:32.

61. Rizvi A, Han D, Danad I, et al.Diagnostic performance of hybrid cardiac imaging methods for assessment of obstructive coronary artery disease compared with stand-alone coronary computed tomography angiography: A meta-analysis. JACC: Cardiovascular Imaging. 2018;11:589–99. [PubMed: 28823745]

62. Nensa F, Poeppel TD, Krings P, Schlosser T. Multiparametric assessment of myocarditis using simultaneous positron emission tomography/magnetic resonance imaging. Eur Heart J. 2014;35:2173-. [PubMed: 24578391]

63. Nensa F, Bamberg F, Rischpler C, et al.Hybrid cardiac imaging using PET/MRI: A joint position statement by the european society of cardiovascular radiology (ESCR) and the european association of nuclear medicine (EANM). European Journal of Hybrid Imaging. 2018;2:14.

64. Kouranos V, Wells A, Sharma R, Underwood S, Wechalekar K. Advances in radionuclide imaging of cardiac sarcoidosis. Br Med Bull. 2015;115. [PubMed: 26585999]

65. Trivieri MG, Dweck MR, Abgral R, et al.18F-sodium fluoride PET/MR for the assessment of cardiac amyloidosis. J Am Coll Cardiol. 2016;68:2712–4. [PubMed: 27978955]

66. Juarez-Orozco LE, Martinez-Manzanera O, Nesterov SV, Kajander S, Knuuti J. The machine learning horizon in cardiac hybrid imaging. European Journal of Hybrid Imaging. 2018;2:15.

67. Slomka PJ, Dey D, Sitek A, Motwani M, Berman DS, Germano G. Cardiac imaging: Working towards fully-automated machine analysis & interpretation. Expert review of medical devices. 2017;14:197–212. [PubMed: 28277804]

68. Cherry SR, Jones T, Karp JS, Qi J, Moses WW, Badawi RD. Total-body PET: Maximizing sensitivity to create new opportunities for clinical research and patient care. J Nucl Med. 2018;59:3–12. [PubMed: 28935835]

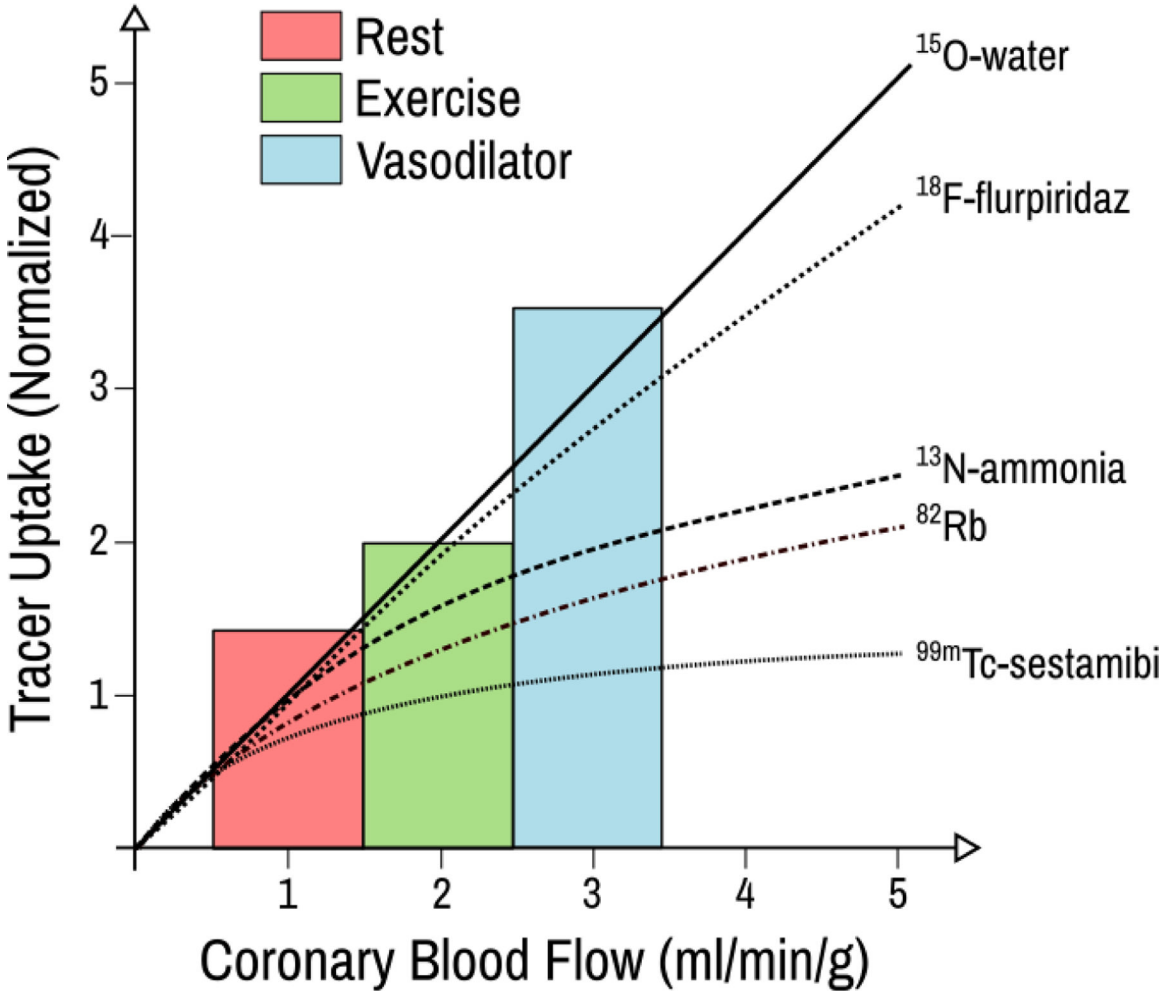

Figure 1: PET and SPECT uptake as a function of coronary blow flow.

PET and SPET radiotracer extraction at different coronary flow rates, including rest, exercise and pharamcologic vasodilation. The bars show the anticipated flow rates for rest, exercise, and vasodilator stress. Figured adapted from (16), licensed under a Creative Commons Attribution 3.0 International License, https://creativecommons.org/licenses/by/3.0/.

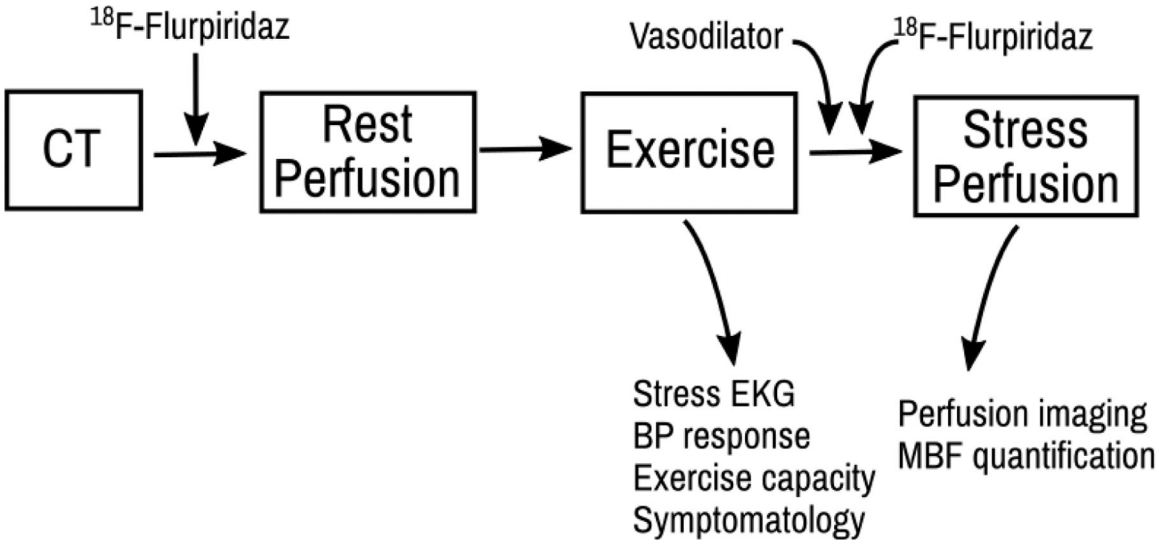

Figure 2: Hybrid exercise-vasodilator stress algorithm.

Proposed hybrid exercise-vasodilator stress algorithm which, when paired with ^{18}F—Flurpiridaz, could enable the collection of both exercise stress information and myocardial blood flow with one clinical study.

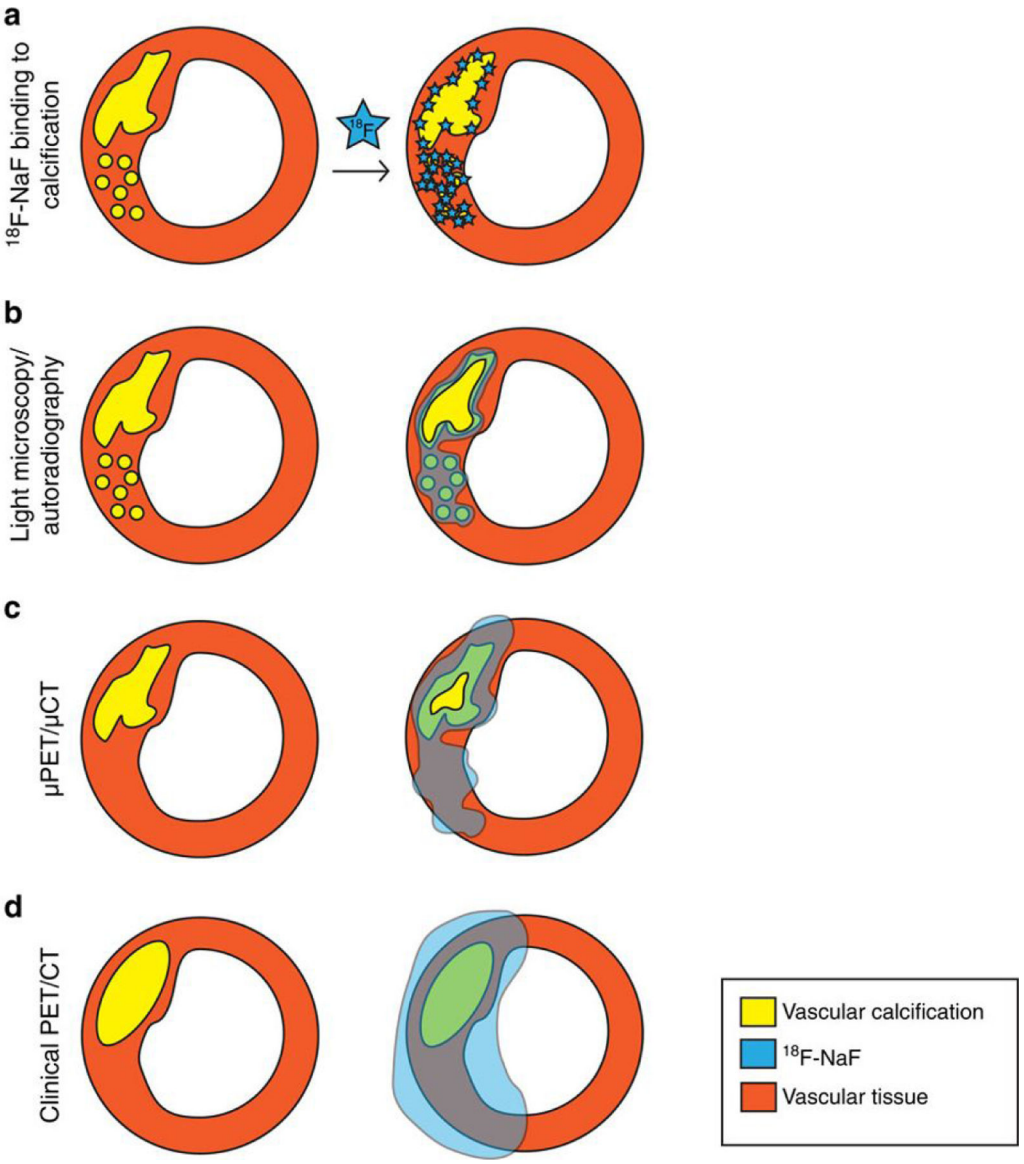

Figure 3: ^{18}F-NaF for non-invasive characterization of coronary plaques.

NaF binds to areas of micro- and macro-calcification within the necrotic core of vascular plaques (row "a"). This property property can be exploited to provide non-invasive, in vivo characterization of coronary plaques with ^{18}F-NaF PET (row "d"). ^{18}F-NaF-avid plaques may be useful for risk stratification and the technique is currently the subject of an ongoing clinical trial. Rows "b" and "c" refer to ex vivo and animal studies, not applicable to patient care. Figure reproduced from (22), licensed under a Creative Commons Attribution 4.0 International License (https://creativecommons.org/licenses/by/4.0/).

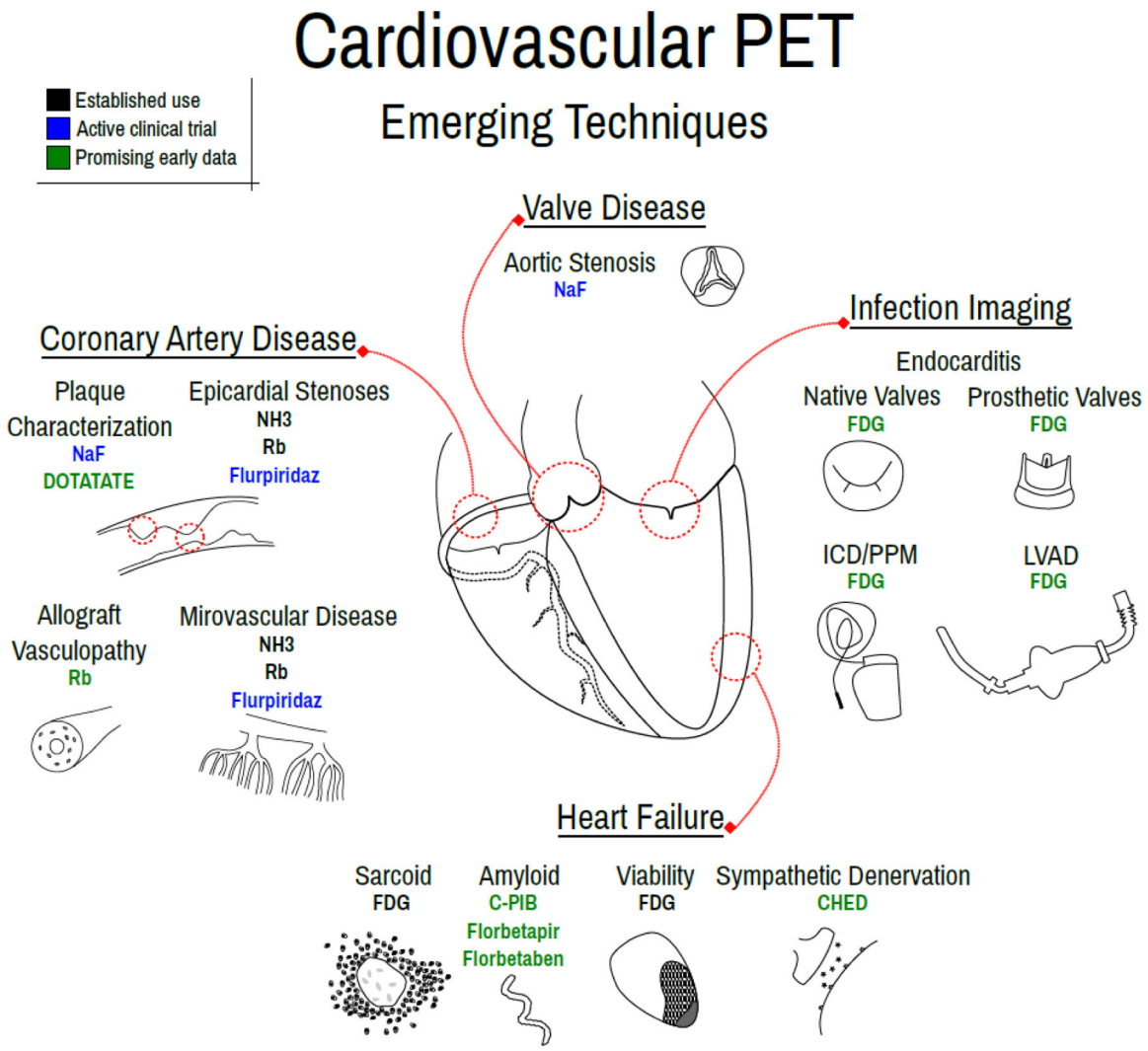

Figure 4: Emerging Techniques of Cardiovascular PET

Emerging techniques of cardiovascular PET, including for valve disease evaluation, coronary artery disease characterization, heart failure assessment and infection imaging.